Int. J. Heat Mass Transfer. Vol. 35, No. 11, pp. 3021–3028, 1992
Printed in Great Britain

0017–9310/92 $5.00 + 0.00

An analytical study on the critical heat flux of countercurrent boiling in a vertical tube with a closed bottom

Y. KATTO and K. WATANABE

Department of Mechanical Engineering, Nihon University, Kanda-Surugadai, Chiyoda-ku, Tokyo 101, Japan

(*Received* 18 *September* 1991)

Abstract—An analytical model is presented for critical heat flux (CHF) in a heated vertical tube connected to a saturated-liquid reservoir at the top and closed at the bottom end. For the liquid film flow subject to both the frictional force of the vapor core flow and that of the tube wall, an equation is derived to estimate the thickness of the liquid film along the tube length. A limit condition is found to appear for the existence of real roots of the equation at the top end of the tube with increasing heat flux, which is caused under the circumstances where the interfacial shear stress exerted by the vapor core flow increases with the liquid film thickness when the vapor flow is turbulent. This limit condition is then shown to agree fairly well with the experimental data of CHF.

1. INTRODUCTION

IN A PREVIOUS study [1], experiments of water boiling in a uniformly heated vertical tube shown in Fig. 1(a) were carried out by distributing 11–17 thermocouples along the tube length, disclosing some peculiar characteristics of critical heat flux (CHF) in this boiling system such as: (i) the onset of the initial abrupt wall-temperature rise is observed not at the bottom end but at an intermediate location of the heated tube; (ii) a considerably long waiting time is often observed before the onset of the initial wall-temperature rise; and (iii) the variation of wall-temperature after the initial temperature rise is rather slow and complicated, in general. These features suggest the need for careful measures in experiments to detect correct values of CHF for this boiling system. Then, in a previous study, a total of 48 data points of CHF were obtained for water boiling within the following experimental range:

$D = 8\,\text{mm}$, $L/D = 38$–113, $P = 101.3$–$198.5\,\text{kPa}$;

and

$D = 10\,\text{mm}$, $L/D = 30$–90, $P = 101.3$–$198.5\,\text{kPa}$.

In the present study, employing new test tubes, additional experiments have been carried out obtaining 49 data points of CHF for water boiling under somewhat extended conditions:

$D = 8\,\text{mm}$, $L/D = 20$–120, $P = 101.3$–$404.2\,\text{kPa}$;

and

$D = 12\,\text{mm}$, $L/D = 60$–80, $P = 101.3$–$198.5\,\text{kPa}$.

Details of the experimental conditions for the water data points mentioned above, together with the vapor/liquid density ratio ρ_v/ρ_L and the Bond number $Bo = [\rho_L g D^2/\sigma]^{1/2}$ are listed in Table 1.

Meanwhile, the experimental conditions of R-113 listed in the bottom two lines of Table 1 are concerned with the data of R-113 measured by Barnard *et al.* [2] and Yokoyama [3] for the same type of boiling system as above. In these two papers, however, the peculiar

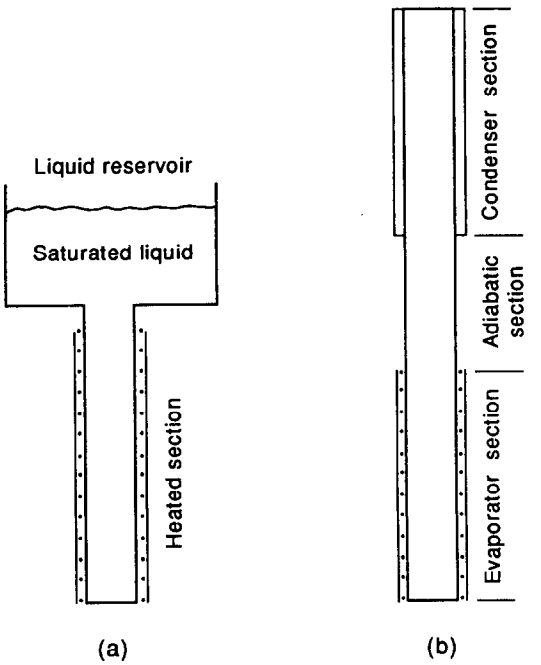

FIG. 1. (a) Vertical tube with a liquid reservoir and a closed bottom. (b) Closed two-phase thermosyphon.

NOMENCLATURE

Bo	Bond number $= (4\rho_L g R^2/\sigma)^{1/2}$
C_{fi}	friction coefficient at vapor/liquid interface
D	tube inside diameter
g	gravitational acceleration
H_{fg}	latent heat of evaporation
L	length of heated tube
m	mass flow rate
P	pressure
q	heat flux
q_c	critical heat flux
R	tube inside radius $= D/2$
Re_{LF}	liquid film Reynolds number
Re_v	Reynolds number of vapor core flow
Re'_v	Reynolds number of vapor core flow defined by relative velocity
u_L	mean velocity of liquid
u_v	mean velocity of vapor
u'	relative velocity between vapor and liquid
z	axial distance from the bottom end.

Greek symbols

Γ	mass flow rate of liquid film per unit tube perimeter
δ	liquid film thickness
μ_L	dynamic viscosity of liquid
ν_v	kinematic viscosity of vapor
ρ_L	liquid density
ρ_v	vapor density
τ_i	shear stress on vapor/liquid interface.

features of CHF such as those mentioned before were not reported, so there may be some questions as to the accuracy of the data; but still a number of thermocouples (5–7 in ref. [2], and 5 in ref. [3]) were employed to detect the onset of the CHF, accordingly the error of the CHF value is presumably restricted in a limited range.

Now, the present study, with the main object of developing an analytical model for CHF in the boiling system of Fig. 1(a), will utilize the above-mentioned data as the basis to confirm the developed model.

With respect to theoretical studies on CHF in similar types of boiling systems to the present one, there have been a few analytical studies on countercurrent annular flow in two-phase closed thermosyphons shown in Fig. 1(b). First, Dobran [4] performed a study taking equations of continuity, motion, and energy into consideration for the liquid film flow, and for the vapor core flow, respectively; and a lumped model was presented assuming a common liquid film thickness δ_m throughout the three sections of the condenser, adiabatic, and evaporator as shown in Fig. 1(b). Reed and Tien [5] then extended the foregoing Dobran's lumped model by assuming a mean liquid film thickness of δ_c, δ_a, and δ_e at the condenser, adiabatic, and evaporator sections, respectively; and a flooding limit is insisted to appear at a section where the calculated rate of change of film thickness with respect to heat input becomes unbounded. A little later, Casarosa and Dobran [6] also reported an analysis of a double-diameter type thermosyphon assuming a mean liquid film thickness of δ_c and δ_a at the condenser and adiabatic sections, respectively.

The present paper, in contrast with the lumped models mentioned above, assumes a continuous variation of the liquid film thickness along the tube length as illustrated in Fig. 2, considering steady-state countercurrent annular flow in the heated tube of Fig. 1(a).

2. ANALYTICAL MODEL

It is assumed in the present study that the liquid film thickness δ is very thin as compared with the tube internal radius R (that is $\delta/R \ll 1$), and that the vapor/liquid density ratio ρ_v/ρ_L is very low (that is, $\rho_v/\rho_L \ll 1$). As to the justification of the former assumption see Section 3.2; and as to the latter assumption, see column ρ_v/ρ_L in Table 1. Furthermore, the effect of inertia is neglected for both the flows of liquid and vapor, and a uniformly heated tube is dealt with for simplicity.

2.1. *Liquid film flow and vapor core flow*

Under steady-state conditions, the upward mass flow rate of vapor m at an arbitrary location z must be equal to the downward mass flow rate of liquid at the same location; and m is given as

$$m = 2\pi R z q / H_{fg} \tag{1}$$

where q is the heat flux, and H_{fg} the latent heat of evaporation. From the assumption $\delta/R \ll 1$, the mean velocity of liquid u_L in the liquid film flow and that of vapor in the vapor core flow u_v can be written as follows:

$$u_L = \frac{m}{\rho_L 2\pi R\delta}, \quad u_v = \frac{m}{\rho_v \pi R^2}. \tag{2}$$

In addition, the relative velocity u' between the liquid and the vapor flow is

$$u' = \left(1 + \frac{\rho_v}{\rho_L}\frac{R}{2\delta}\right)u_v. \tag{3}$$

Meanwhile, the mass flow rate Γ in the liquid film per unit tube perimeter is

$$\Gamma = m/(2\pi R). \tag{4}$$

Table 1. Experimental conditions of CHF data, prediction accuracy, and calculted values of δ/R, Re_v, Re'_v, Re_{LF}, $q_c \cdot (L/D)$

No.	Fluid	Data sources	Data points	D (mm)	P (kPa)	L/D	ρ_v/ρ_L	Bo	$\mu(r)$	$\sigma(r)$	δ/R (%)	Re_v	Re'_v	Re_{LF}	$q_c \cdot (L/D)$ ($\times 10^6$)
1	Water	[1]†	27	8.0	101.3	20.0–120.0	0.00062	3.20	1.011	0.084	3.65–4.15	5410–5550	5430–5570	239–239	4.68–4.81
2	Water	[1]†	27	8.0	198.5	20.0–120.0	0.00119	3.28	1.005	0.079	4.04–4.15	6120–9180	6150–6220	345–345	5.46–5.52
3	Water	[1]†	15	8.0	404.2	20.0–120.0	0.00238	3.40	1.014	0.063	4.10–4.20	6870–6940	6950–7020	504–504	6.37–6.44
4	Water	[1]†	12	10.0	101.3	30.0–90.0	0.00062	3.99	0.980	0.069	3.59–4.15	6690–6750	6710–6780	293–293	4.63–4.68
5	Water	[1]†	12	10.0	198.5	30.0–90.0	0.00119	4.10	1.050	0.064	3.60–3.70	7590–7610	7630–7660	425–425	5.42–5.44
6	Water	[1]†	2	12.0	101.3	60.0–80.0	0.00062	4.79	1.028	0.001	3.25–3.25	7910–7910	7930–7940	344–344	4.56–4.57
7	Water	[1]†	2	12.0	198.5	60.0–80.0	0.00119	4.92	1.062	0.001	3.30–3.35	9000–9000	9050–9060	503–503	5.36–5.36
		Subtotal 97							1.012	0.076					
8	R-113	[3]	32	8.5	101.3	18.8–112.9	0.00495	8.54	0.751	0.076	4.90	12400	12700	270	0.561
9	R-113	[2]	9	17.22	101.3	8.7–58.1	0.00495	17.3	1.171	0.242	3.55	29470	30200	641	0.658
		Subtotal 41							0.844	0.218					

† The present study.

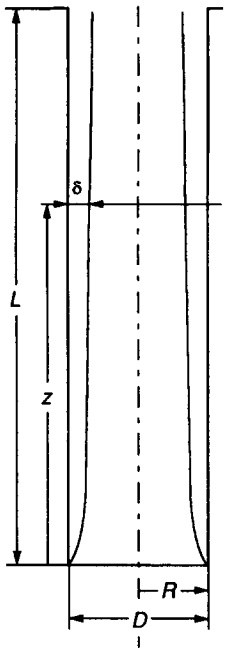

FIG. 2. Countercurrent annular flow in a heated vertical tube with a closed bottom.

Then, the film Reynolds number for the liquid film flow Re_{LF}, and the absolute and the relative Reynolds number Re_v and Re'_v for the vapor core flow, respectively, are given as follows:

$$Re_{LF} = \frac{4\Gamma}{\mu_L}, \quad Re_v = \frac{u_v 2R}{\nu_v}, \quad Re'_v = \frac{u' 2R}{\nu_v}. \tag{5}$$

2.2. *Governing equation of liquid film thickness*

Since it has been assumed that $\delta/R \ll 1$ and that inertia is neglected, if the liquid film flow is laminar, one can make the same analysis as that of Nusselt for the liquid film flow on a vertical flat wall. For the local downward velocity u at the normal distance y from the wall, the following differential equation is readily derived:

$$\mu_L \frac{d^2u}{dy^2} + \rho_L g = 0 \tag{6}$$

where μ_L is the dynamic viscosity of liquid, and g is the gravitational acceleration. Integrating this equation under boundary conditions that $u = 0$ at $y = 0$ and that $\mu_L du/dy = -\tau_i$ at $y = \delta$ (where τ_i is the shear stress exerted by the vapor core flow on the vapor/liquid interface), it immediately gives the following relationship between Γ and δ:

$$\frac{\delta}{R} = \frac{3\Gamma\mu_L}{\rho_L^2 g \delta^2 R} + \frac{3}{2}\frac{\tau_i}{\rho_L g R}. \tag{7}$$

Since the magnitude of the film Reynolds number Re_{LF} is very low within the experimental range of Table 1, as will be described later in Section 3.2, there

is no need to consider turbulent liquid film flow in the present study.

2.3. *Magnitude of interfacial shear stress*

For the relative velocity u' between the liquid and the vapor flow, the interfacial shear stress τ_i is given as

$$\tau_i = \tfrac{1}{2}\rho_v(u')^2 C_{fi} \tag{8}$$

where C_{fi} is the friction coefficient. Following Dobran [4] and Reed and Tien [5], expressions of C_{fi} are as follows:

For laminar vapor core flow

$$C_{fi} = (16/Re'_v)[\phi/(e^{\phi}-1)] \tag{9}$$

where $\phi = (q/H_{fg})R/(4\mu_L)$, a correction factor as suggested by Blangetti and Naushahi [7] accounting for the influence of interfacial mass flux. Within the range of the present study, the effect of ϕ is not large.

For turbulent vapor core flow

$$C_{fi} = 0.005 + x_1(\delta/R)^{x_2} \tag{10}$$

where

$$x_1 = 0.2574(Bo/2)^{x_2}\cdot 10^{9.07/Bo},$$

and

$$x_2 = 1.63 + 4.74/Bo.$$

Equation (10) is the correlation of C_{fi} presented by Bharathan *et al.* [8].

Now, as for the magnitude of C_{fi} in the transition region between laminar and turbulent vapor core flow, its continuous change is assumed in this study as follows:

$$\left.\begin{aligned}&\text{For } 2900 < Re'_v < 11\,000,\\ &\frac{C_{fi}-C_{fi(9)}}{0.8C_{fi(10)}-C_{fi(9)}} = \frac{Re'_v-2900}{11\,000-2900}\\ &\text{and for } 11\,000 < Re'_v < 20\,000\\ &\frac{C_{fi}-0.8C_{fi(10)}}{C_{fi(10)}-0.8C_{fi(10)}} = \frac{Re'_v-11\,000}{20\,000-11\,000}\end{aligned}\right\} \tag{11}$$

where $C_{fi(9)}$ is the value of C_{fi} of equation (9) at $Re'_v = 2900$, and $C_{fi(10)}$ is the value of C_{fi} of equation (10) which is independent of Re'_v. The extent of the above-mentioned transition region, $Re'_v = 2900$–$20\,000$, is comparable with that of single-phase flow in tubes with very high surface-roughness (cf. Fig. 20.17 of ref. [9], for example). In addition to this, it must be noted that, in the present case, the magnitude of Re'_v increases with the increase of the length z in Fig. 2, so the feature of transition from laminar to turbulent flow may somewhat differ from the ordinary case where Re'_v is kept constant along the tube length.

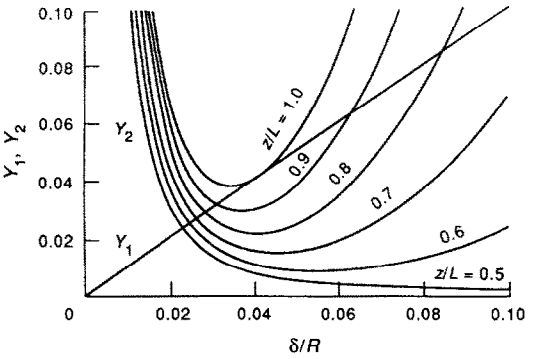

FIG. 3. Variation of the Y_2–δ/R curve with axial location z/L (water, $D = 8$ mm, $L/D = 25$, $P = 101.3$ kPa, $q = 190\,600$ W m^{-1}).

2.4. *Limit for the existence of real root of equation* (7)

Substituting Γ of equations (4) and τ_i of equation (8) into the right-hand side of equation (7), the liquid film thickness δ at an arbitrary location z along the tube length can be estimated. In order to see this situation, let Y_1 and Y_2 represent the left-hand and the right-hand sides of equation (7), respectively, as

$$Y_1 = \frac{\delta}{R} \tag{12}$$

$$Y_2 = \frac{3\Gamma\mu_L}{\rho_L^2 g\delta^2 R} + \frac{3}{2}\frac{\tau_i}{\rho_L g R} \tag{13}$$

and the calculated values of Y_1 and Y_2 against δ/R have a mutual relationship, shown in Fig. 3, where an intersection point between the Y_1- and Y_2-line corresponds to a solution of equation (7) as to the liquid film thickness δ.

It is noticed here that only one intersection appears at low values of z/L, while two intersections appear at high values of z/L being accompanied by a limit condition at $z/L = 1.0$. Relating to this, it is helpful to see the situation of Fig. 4 which represents the

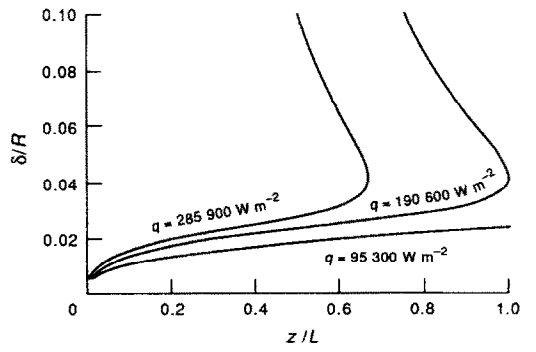

FIG. 4. Variation of the liquid film thickness along the tube length (water, $D = 8$ mm, $L/D = 25$, $P = 101.3$ kPa).

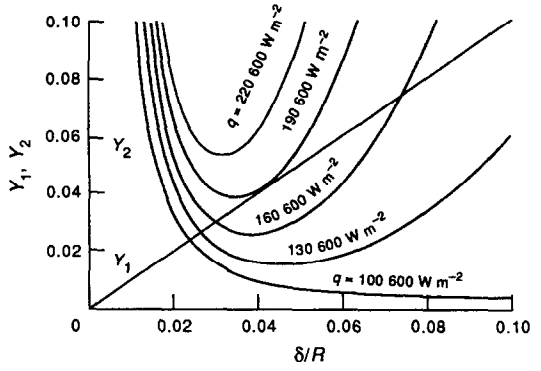

FIG. 5. Variation of the Y_2–δ/R curve with heat flux q at the top end of the tube (water, $D = 8$ mm, $L/D = 25$, $P = 101.3$ kPa).

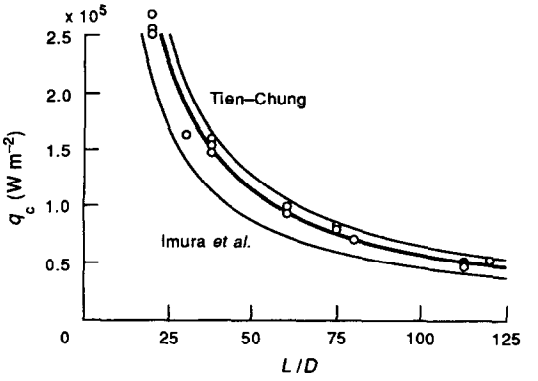

FIG. 7. Comparison of measured and predicted CHF (water, $D = 8$ mm, $P = 198.5$ kPa).

continuous variation of δ along the tube length for three different values of heat flux q. It is known from Fig. 4 that (i) when there are two intersections between Y_1 and Y_2 in Fig. 3, δ of low value among the two is realized, and that (ii) for a heat flux q higher than a definite value (190 600 W m^{-1} in the case of Fig. 4), no steady-state liquid film flow can exist at and near the top end of the heated tube.

Now, Fig. 5 represents the relationship between Y_1 and Y_2 at the top end of the tube ($z/L = 1$) for various values of q, showing that the value of $q = 190\,600$ W m^{-1} in case of Fig. 4 is the limit for the existence of real root δ, that is the existence of the steady-state liquid film flow, at the top end of the tube.

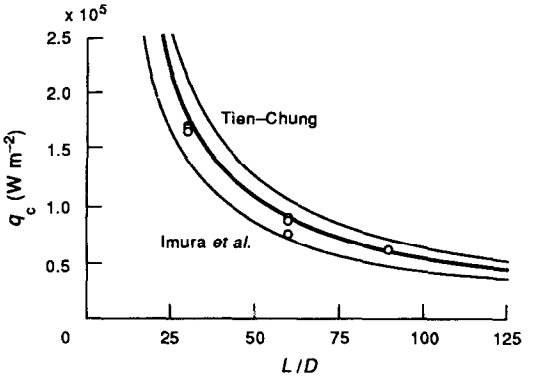

FIG. 8. Comparison of measured and predicted CHF (water, $D = 10$ mm, $P = 198.5$ kPa).

3. CRITICAL HEAT FLUX

3.1. *Comparison of predicted and measured CHF*

Typical experimental CHF data are plotted in Figs. 6–9 for water, and in Figs. 10 and 11 for R-113. Two thin lines entered in each figure represent the following empirical correlations of CHF proposed by Tien and Chung [10], and Imura *et al.* [11], respectively, for two-phase closed thermosyphon of Fig. 1(b):

Tien and Chung

$$\frac{q_c}{\rho_v H_{fg}} \Big/ \left[\frac{\sigma g(\rho_L - \rho_v)}{\rho_v^2}\right]^{1/4} = \frac{3.2}{4} \frac{1}{[1+(\rho_v/\rho_L)^{1/4}]^2 (L/D)} \tag{14}$$

and Imura *et al.*

$$\frac{q_c}{\rho_v H_{fg}} \Big/ \left[\frac{\sigma g(\rho_L - \rho_v)}{\rho_v^2}\right]^{1/4} = 0.16 \frac{1}{(L/D)(\rho_v/\rho_L)^{0.13}}. \tag{15}$$

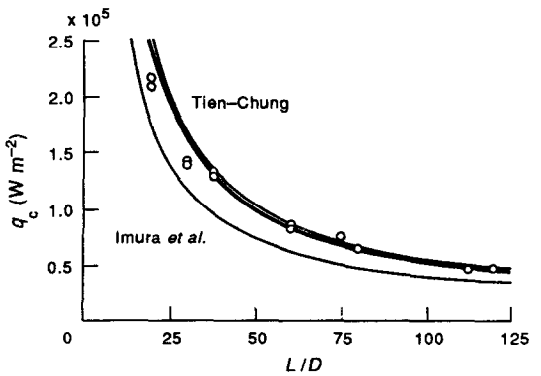

FIG. 6. Comparison of measured and predicted CHF (water, $D = 8$ mm, $P = 101.3$ kPa).

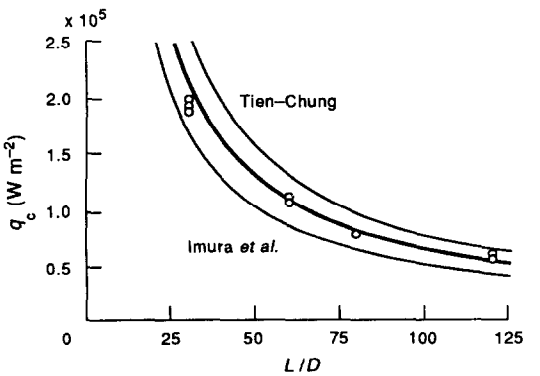

FIG. 9. Comparison of measured and predicted CHF (water, $D = 8$ mm, $P = 404.2$ kPa).

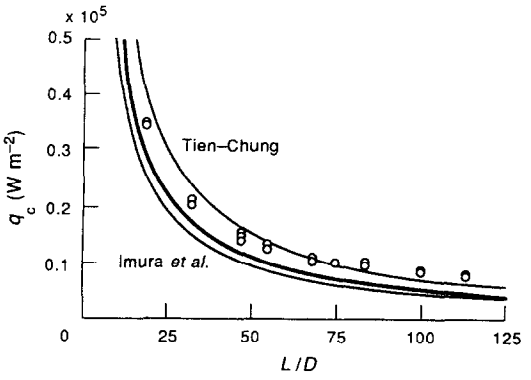

FIG. 10. Comparison of measured and predicted CHF (R-113, $D = 8.5$ mm, $P = 101.3$ kPa).

The original correlation of Tien and Chung includes a correction term relating to the effect of the Bond number Bo, but it has been omitted from equation (14) because of better correspondence to the present data for the boiling system of Fig. 1(a). Anyhow, approximately speaking, a trend is observed in that the data points of CHF in Figs. 6–11 appear in a region between the two empirical correlations.

Meanwhile, a thick line in each figure represents the value of CHF predicted by the analytical model, that is the limit for the existence of real root δ of equation (7) at the top end of the tube. It agrees well with the measured data for water (Figs. 6–9). As for R-113 (Figs. 10 and 11), some deviation is observed but the agreement with the data is not too bad.

In columns $\mu(r)$ and $\sigma(r)$ in Table 1 the statistical prediction accuracy for each group of experimental data are listed, where r represents

$$r = (\text{predicted CHF})/(\text{measured CHF})$$

and $\mu(r)$ and $\sigma(r)$ are the mean value and the standard deviation of r, respectively.

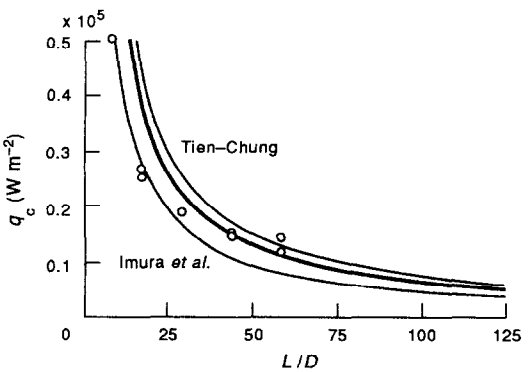

FIG. 11. Comparison of measured and predicted CHF (R-113, $D = 17.22$ mm, $P = 101.3$ kPa).

3.2. *Remarks on the state of flow at the CHF condition*

According to the analytical model proposed in the present study, the following features are suggested for the flow configuration relating to the onset of the CHF condition at the top end of the tube.

(i) The magnitude of δ/R is within the range of 0.0325–0.0490 as seen in Table 1, which means that the error does not exceed 4.9% with respect to the basic assumption $\delta/R \ll 1$ on which the present analysis has been made.

(ii) The magnitude of the film Reynolds number Re_{LF}, 239–641 as seen in Table 1, is low enough to satisfy the assumption of laminar liquid film flow adopted in the present model.

(iii) As for the vapor core flow, the relative Reynolds number Re'_v has been discriminated from the absolute Reynolds number Re_v in this study. Actually, however, their quantitative difference is very small being less than 2.5% within the experimental range of Table 1.

(iv) It is noticed from Figs. 3 and 5 that CHF occurs only when the Y_2–δ/R curve is downwardly convex, because this state can lead to a limit for the existence of real root δ/R.

Now it is clear that the first term on the right-hand side of equation (13) always decreases with increasing δ. Meanwhile, the second term is nearly independent of δ if the vapor core flow is laminar, because the effect of δ on τ_i brought about by equations (8) and (9) is very slight since the quantitative difference between Re'_v and Re_v, and hence between u' and u_v, is negligibly small [cf. the preceding item (iii)]. This means that either the Y_2–δ/R curve at $z/L = 0.5$ in Fig. 3 or that at $q = 100\,600$ W m^{-1} in Fig. 5 corresponds to laminar vapor core flow.

However, when the vapor mass flow rate is increased up to enter the transition region toward the turbulent flow, or the region of turbulent flow itself, the magnitude of τ_i increases noticeably with δ under the influence of the term $x_1(\delta/R)^{x_2}$ included in equation (10); and this is the reason why the Y_2–δ/R curve becomes downwardly convex for $z/L > 0.6$ in Fig. 3, and for $q > 130\,600$ W m^{-1} in Fig. 5, respectively.

That is to say, CHF in the present boiling system is generated by the interfacial shear stress τ_i which increases with the liquid film thickness δ when the vapor core flow is turbulent. This nature of τ_i is observed not only in equation (10) employed in this study but also in other empirical correlations of τ_i proposed by Wallis [12], Whalley and Hewitt [13], and others.

(v) In the present analytical model, heat flux q has its role at two places: the right-hand side of equation (1), and ϕ of equation (9). Under such circumstances, the following analysis can be made with respect to the characteristics of the value of CHF.

First, if $Re'_v > 11\,000$, equation (11) suggests that C_{ti} is unaffected by ϕ of equation (9). This means that the CHF condition can be determined relating to only the magnitude of Lq_c [consider $z = L$ in equation (1)],

which results in the fact that, on the bottom two lines of Table 1, each magnitude of δ/R, Re_v, Re'_v, Re_{LF}, and $q_c \times (L/D)$ has been determined irrespectively of the variation of L under a fixed condition of D.

Second, if $Re'_v < 11\,000$, C_{fi} is subject to the influence of ϕ, so the above-mentioned five quantities disperse in magnitude depending on L as seen in Table 1. However, the degree of the dispersion is very small: even for the most dispersible case of the top line of Table 1 where the magnitude of Re'_v is minimal, the dispersion of the value of $q_c \times (L/D)$ is only 2.8%.

Hence, it can be assumed without serious error that the magnitude of q_c is inversely proportional to the tube length L, irrespective of Re'_v, under a fixed condition of D within the present experimental range.

4. CONCLUSIONS

Based on a total of 97 CHF data points obtained in the previous and present papers for water and a total of 41 data points found in the literature for R-113 in the boiling system of Fig. 1(a), in the experimental ranges of Table 1, an analytical model of CHF has been presented.

Assuming steady-state countercurrent annular flow in a uniformly heated vertical tube, a governing equation is derived for laminar liquid film flow to estimate the liquid film thickness δ at the top end of the tube.

A limit for the existence of the real root of the foregoing equation is then found to appear at a definite value of heat flux, and it is shown that the limit agrees fairly well with the experimental CHF data.

In addition, the following matters are disclosed: (i) the CHF in the present boiling system is generated through the interfacial shear stress τ_i which increases with the liquid film thickness when the vapor core flow is turbulent; (ii) within the experimental range of Table 1, the liquid film flow is very thin to be less than 4.9% of the tube radius R, and is always laminar; and (iii) approximately speaking, the critical heat flux q_c can be regarded as being inversely proportional to the tube length L under a fixed condition of the tube diameter D.

REFERENCES

1. Y. Katto and T. Hirao, Critical heat flux of counter-flow boiling in a uniformly heated vertical tube with a closed bottom, *Int. J. Heat Mass Transfer* **34,** 993–1001 (1991).
2. D. A. Barnard, F. R. Dell and R. A. Stinchcombe, Dry-out at low mass velocities for an upward boiling flow of Refrigerant-113 in a vertical tube, UKAEA, AERE-R 7726 (1974).
3. M. Yokoyama, A study of CHF in countercurrent two-phase flow in vertical tubes, M.Sc. thesis, Department of Mechanical Engineering, Nihon University (1986).
4. F. Dobran, Steady-state characteristics and stability thresholds of a closed two-phase thermosyphon, *Int. J. Heat Mass Transfer* **28,** 949–957 (1985).
5. J. G. Reed and C. L. Tien, Modeling of the two-phase closed thermosyphon, *Trans. ASME, J. Heat Transfer* **109,** 722–730 (1987).
6. C. Casarosa and F. Dobran, Experimental investigation and analytical modeling of a closed two-phase thermosyphon with imposed convection boundary conditions, *Int. J. Heat Mass Transfer* **31,** 1815–1833 (1988).
7. F. Blangetti and M. Naushahi, Influence of mass transfer on the momentum transfer in condensation and evaporation phenomena, *Int. J. Heat Mass Transfer* **23,** 1694–1695 (1980).
8. D. Bharathan, G. B. Wallis and H. J. Richter, Air–water countercurrent annular flow, EPRI Report NP-1165 (1979).
9. H. Schlichting (translated by J. Kestin), *Boundary Layer Theory*, p. 418. Pergamon Press, London (1955).
10. C. L. Tien and K. S. Chung, Entrainment limits in heat pipes, *AIAA J.* **17,** 643–646 (1978).
11. H. Imura, K. Sasaguchi and H. Kozai, Critical heat flux in a closed two-phase thermosyphon, *Int. J. Heat Mass Transfer* **26,** 1181–1188 (1983).
12. G. B. Wallis, Annular two-phase flow: part 2, additional effects, *Trans. ASME, J. Basic Engng* **92,** 73–82 (1970).
13. P. B. Whalley and G. F. Hewitt, The correlation of liquid entrainment fraction and entrainment rate in annular two-phase flow, UKAEA, AERE 9187 (1978).

ETUDE ANALYTIQUE DU FLUX THERMIQUE CRITIQUE DE L'EBULLITION A CONTRE-COURANT DANS UN TUBE VERTICAL AVEC LA BASE FERMEE

Résumé—On présente un modèle analytique pour le flux thermique critique (CHF) dans un tube vertical relié à la partie supérieure à un réservoir saturé et ayant l'extrémité inférieure fermée. Pour le liquide s'écoulant en film soumis à la fois à la force de frottement avec le noyau de vapeur et avec la paroi, on donne une équation pour estimer l'épaisseur du film liquide le long du tube. Une condition aux limites apparaît pour l'existence des racines réelles de l'équation au sommet du tube avec un flux thermique croissant, l'effet de cisaillement à l'interface augmentant avec l'épaisseur du film liquide dans le cas de l'écoulement turbulent de la vapeur. Cette condition aux limites s'accorde très bien avec les données expérimentales de CHF.

ANALYTISCHE UNTERSUCHUNG DER KRITISCHEN WÄRMESTROMDICHTE BEI GEGENSTROMVERDAMPFUNG IN EINEM SENKRECHTEN ROHR MIT GESCHLOSSENEM BODEN

Zusammenfassung—Es wird ein analytisches Modell für die kritische Wärmestromdichte in einem senkrechten Rohr vorgestellt. Das Rohr ist am oberen Ende mit einem Reservoir gesättigter Flüssigkeit verbunden und am unteren Ende verschlossen. Am strömenden Flüssigkeitsfilm greifen die Reibungskräfte der Dampfströmung im Kern und diejenigen an der Wand an. Für die Dicke des Flüssigkeitsfilms entlang der Rohrlänge wird eine Gleichung formuliert. Bei zunehmender Wärmestromdichte gibt es eine Grenzbedingung für die Existenz realer Lösungen der Gleichung. Sie wird erreicht, wenn die durch den Dampf bei turbulenter Strömung bewirkte Schubspannung an der Phasengrenze mit der Filmdicke zunimmt. Es wird gezeigt, daß diese Grenzbedingung gut mit den gemessenen kritischen Wärmestromdichten übereinstimmt.

АНАЛИТИЧЕСКОЕ ИССЛЕДОВАНИЕ КРИТИЧЕСКОГО ТЕПЛОВОГО ПОТОКА ПРИ КИПЕНИИ В СЛУЧАЕ ПРОТИВОТОЧНОГО ТЕЧЕНИЯ В ВЕРТИКАЛЬНОЙ ТРУБЕ С ЭАКРЫТЫМ НИЖНИМ ТОРЦОМ

Аннотация—Представлена аналитическая модель для критического теплового потока (КТП) в нагреваемой вертикальной трубе, верхний торец которой соединен с резервуаром с насыщенной жидкостью, а нижний закрыт. Для пленочного течения жидкости, на которое воздействуют силы трения на границах с паровым ядром и стенкой трубы, получено уравнение, позволяющее оценить толщину жидкой пленки по длине трубы. Найдено, что в случае увеличения касательного напряжения на границе с паровым ядром по мере роста толщины пленки при турбулентном течении пара имеет место предельное условие существования действительных корней соответствующего уравнения. Показано, что это предельное условие достаточно хорошо согласуется с экспериментальными данными по КТП.